AIP Journal of Applied Physics

Charge neutral MoS2 field effect transistors through oxygen plasma treatment

Rohan Dhall, Zhen Li, Ewa Kosmowska, and Stephen B. Cronin

Citation: Journal of Applied Physics **120**, 195702 (2016); doi: 10.1063/1.4967398
View online: http://dx.doi.org/10.1063/1.4967398
View Table of Contents: http://scitation.aip.org/content/aip/journal/jap/120/19?ver=pdfcov
Published by the AIP Publishing

Charge neutral MoS_2 field effect transistors through oxygen plasma treatment

Rohan Dhall,[1] Zhen Li,[1] Ewa Kosmowska,[2] and Stephen B. Cronin[1]
[1]*Ming Hsieh Department of Electrical Engineering, University of Southern California, Los Angeles, California 90089, USA*
[2]*XEI Scientific, Redwood City, California 94063, USA*

(Received 30 May 2016; accepted 27 October 2016; published online 18 November 2016)

Lithographically fabricated MoS_2 field effect transistors suffer from several critical imperfections, including low sub-threshold swings, large turn-on gate voltages (V_T), and wide device-to-device variability. The large magnitude and variability of V_T stems from unclean interfaces, trapped charges in the underlying substrate, and sulfur vacancies created during the mechanical exfoliation process. In this study, we demonstrate a simple and reliable oxygen plasma treatment, which mitigates the effects of unintentional doping created by surface defect sites, such as S vacancies, and surface contamination. This plasma treatment restores charge neutrality to the MoS_2 and shifts the threshold turn-on voltage towards 0 V. Out of the 10 devices measured, all exhibit a shift of the FET turn-on voltage from an average of −18 V to −2 V. The oxygen plasma treatment passivates these defects, which reduces surface scattering, causing increased mobility and improved sub-threshold swing. For as-prepared devices with low mobilities (~0.01 cm^2/V s), we observe up to a 190-fold increase in mobility after exposure to the oxygen plasma. Perhaps the most important aspect of this oxygen plasma treatment is that it reduces the device-to-device variability, which is a crucial factor in realizing any practical application of these devices. *Published by AIP Publishing.* [http://dx.doi.org/10.1063/1.4967398]

INTRODUCTION

The unique properties of two dimensional materials have attracted a lot of interest for their potential applications in electronic and optoelectronic devices.[1–5] While the high carrier mobility of graphene[6] makes it an attractive material as a possible transparent electrode, it is of limited value for optoelectronics and digital logic due to its gapless electronic band structure. Transition metal dichalcogenides (TMDCs), such as MoS_2, WSe_2, and WS_2, are now being explored as possible alternatives for optoelectronic materials due to their finite band gaps, which lie in the visible range of the electromagnetic spectrum.[7–10] Monolayer MoS_2 is a direct band gap semiconductor,[1,5,10] and hence, desirable for applications in optoelectronic devices, such as light emitting diodes (LEDs). Atomically thin MoS_2 field effect transistors (FETs) have also been demonstrated by several research groups. However, the utility of MoS_2 in high performance electronics is fundamentally limited. As pointed out by Yoon *et al.*,[11] the carrier mobility in MoS_2 is limited by its relatively heavy electron mass ($0.45m_o$), and it is unlikely to be able to compete with the state-of-the-art III–V transistors. To further complicate matters, surface contamination and substrate interactions further degrade carrier mobilities in these two dimensional material systems. Nevertheless, considerable effort has gone into schemes to produce higher mobility MoS_2 FETs. For instance, Radisavljevic *et al.* showed improved field effect transistor (FET) mobilities in single layer MoS_2 transistors achieved by high temperature annealing and by using a dielectric coating of HfO_2 to passivate the MoS_2 surface.[4] Other studies have utilized hexagonal boron nitride encapsulation for enhanced mobility MoS_2 FET devices.[12–16] In our previous work, we reported an oxygen plasma treatment that improved the luminescence efficiency of few-layer MoS_2 by up to 20-fold due to an indirect-to-direct bandgap transition.[17] More recently, Ali Javey's group reported an air-stable, solution-based chemical treatment using an organic non-oxidizing superacid (bis(trifluoromethane) sulfonimide (TFSI)), which uniformly enhances the photoluminescence and minority carrier lifetime of monolayer MoS_2 by more than two orders of magnitude.[18] Currently, lithographically fabricated MoS_2 transistors suffer from two imperfections detrimental to low power CMOS applications: (1) the large turn-on gate voltages (V_T) needed to switch the transistor state and (2) severely degraded sub-threshold swing. The origin of both these imperfections can be traced back to the high density of interface trap charges and substrate interactions. In particular, the large turn-on voltages in MoS_2-based FETs arise due to Sulphur vacancies, which are known to inherently *n*-dope the MoS_2 channel, moving it away from charge neutrality.[19]

In the work presented here, we show that the controlled exposure to a downstream (remotely generated) oxygen plasma dramatically improves the measured transport (*I–V*) characteristics. The turn-on voltage (V_T) moves closer to zero gate voltage due to screening of charged impurities, and a reduction of the sub-threshold voltage swing is observed. Typically, devices fabricated in this study exhibit carrier mobilities (~1–10 cm^2/V s) near typically reported values in literature. On occasion however, a fabricated device may yield rather low mobility. In such rare cases, where the device mobility is remarkably low (~0.01 cm^2/V s), likely limited by impurity scattering, we see a dramatic (up to

190-fold) improvement in carrier mobilities. These lower mobility, as-fabricated devices tend to have a layer thickness <5 layers, making them more susceptible to scattering from surface impurities. After plasma treatment, these defective devices are also restored to moderate device performance.

EXPERIMENTAL DETAILS

We mechanically exfoliate MoS_2 onto a pre-cleaned Si/SiO_2 wafer. Few-layer (3–15 layers) flakes are located using optical microscopy, and Ti (5 nm)/Au (50 nm) source and drain electrodes are patterned using electron beam lithography, as shown in Figure 1. The underlying silicon is used to provide a back gate for the sample, as illustrated in the schematic diagram in Figure 1(a). Following device fabrication, transport characteristics (i.e., current-gate voltage curves) are measured using a probe station under ambient conditions. The device is then exposed to a remotely generated oxygen plasma as described below, and the transport measurements are repeated on the same device. The plasma used for the cleaning process is remotely generated using ambient air with 20 W of RF power, and the sample is placed in a chamber (XEI Scientific Evactron) at 200 mTorr, about 10 cm upstream from the plasma source, for 2 min. The downstream (or remote) generation of plasma is crucial to minimizing direct bombardment of the MoS_2 by ionic species accelerated in an electric field. In this way, one ensures that the removal of impurities and surface contaminants is driven by the chemical reactivity of the oxygen radicals, rather than an unselective physical bombardment process. The air generated plasma, as used in this study, typically comprises of electrons, nitrogen, and oxygen ions, as well as neutral oxygen radicals.

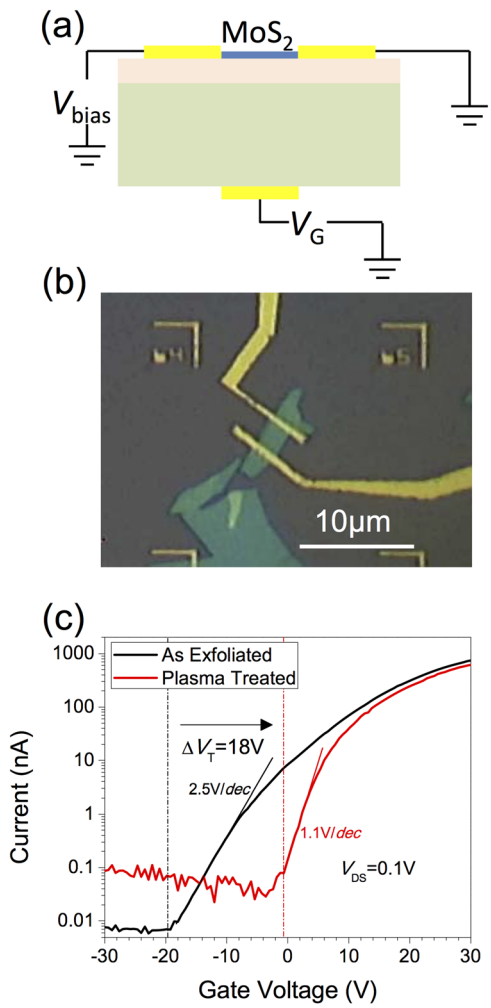

FIG. 1. (a) Schematic diagram and (b) optical microscope image of a back-gated MoS_2 FET device. (c) A log-linear plot of the source-drain current as a function of the applied gate voltage.

RESULTS AND DISCUSSIONS

In Figure 1(c), the source-drain current (I_D) is plotted on a log scale as a function of the applied gate voltage V_G. The device shows *n*-type conductance at positive applied gate voltages, and is turned off at negative gate voltages. The devices also exhibit a linear dependence of current on the applied source-drain bias voltages (as shown in Figure S1 of the supplementary material), which indicates that Ohmic contacts are made with the metal contacts. This particular device shows a shift of the turn-on voltage from −19.4 V to −0.9 V after exposure to the remote oxygen plasma. For the 10 FET devices measured in this study, we observe a shift in the turn-on voltage from an average of −18 V to −2 V, as summarized in Table I. As mentioned before, the large magnitude of the turn-on voltage arises due to the abundance of sulphur vacancies in mechanically exfoliated MoS_2, and this has been reported previously by various groups[19] (see Table S1). The plasma is comprised of charged ions and neutral O

TABLE I. The FET carrier mobilities (μ) and turn-on voltages (V_T) for 10 MoS_2 FET devices before and after remote oxygen plasma treatment with layer thickness more than five layers.

Device	V_T (Pre) (V)	V_T (Post) (V)	ΔV_T (V)	μ_{pre} (cm^2/V s)	μ_{post} (cm^2/V s)	μ_{post}/μ_{pre}
1	−14	−3	11	51.4	21.79	0.4
2	−20	6	26	22.1	5.72	0.3
3	−16	−12	4	45.5	24.69	0.5
4	−17	0.5	17.5	29.6	5.51	0.2
5	−19.5	−6	13.5	38.9	13.38	0.3
6	−18	2	20	19.8	16.64	0.8
7	−18	−2	16	25.4	21.00	0.8
8	−22	−6	16	26.6	12.50	0.5
9	−20	−3	17	25.5	15.65	0.6
10	−15	0	15	18.0	14.31	0.8
	−17.95	−2.35	15.6	30.3	15.1	0.53

TABLE II. The FET carrier mobilities (μ) and turn-on voltages (V_T) for 3 MoS_2 FET devices before and after remote oxygen plasma treatment with layer thickness less than five layers.

Device	V_T (Pre) (V)	V_T (Post) (V)	ΔV_T (V)	μ_{pre} (cm^2/V s)	μ_{post} (cm^2/V s)	μ_{post}/μ_{pre}
1	−20	−4	16	0.017	3.21	192
2	−19	4	23	0.001	0.02	15.0
3	−18	1.5	19.5	0.002	0.03	18.4
Avg	−19	0.5	**19.5**	0.007	1.08	**75.1**

radicals that bind readily to S-vacancies and form covalent bonds with the Mo atoms, since O has the same valence number as S, thus mitigating the doping effects associated with the vacancy. In fact, O has a slightly higher electronegativity than S and will bind more strongly than a corresponding S atom.

It should be noted that the results obtained here using a remotely generated oxygen plasma stand in contrast to those obtained utilizing a conventional local O_2 plasma. Islam *et al*. reported the destructive effects of oxygen plasma exposure to the surface of MoS_2, showing a severe degradation of the FET mobility after just a few seconds of exposure to the locally generated oxygen plasma.[20] In contrast, using the gentler, remotely generated O_2 plasma, we typically observe only a slight degradation of carrier mobility, despite using considerably longer exposure times (approximately 3 min). However, sample degradation is a more significant factor for monolayer and bilayer flakes.

Our initial intent was to use this oxygen plasma to selectively remove the surface residue created during the lithographic process. The AFM images in Figure 2 show an exfoliated MoS_2 flake before and after oxygen plasma treatment. Before plasma treatment, this flake exhibits substantial surface residues left over from the lithographic processes (i.e., ethyl lactate-6, PMMA 950 C2, acetone, isopropanol). It is also possible that the tape residue from the mechanical exfoliation process also contributes to this unwanted surface contamination on the MoS_2 flake. After plasma cleaning, a majority of this residue is removed, without damaging the MoS_2 flake itself.

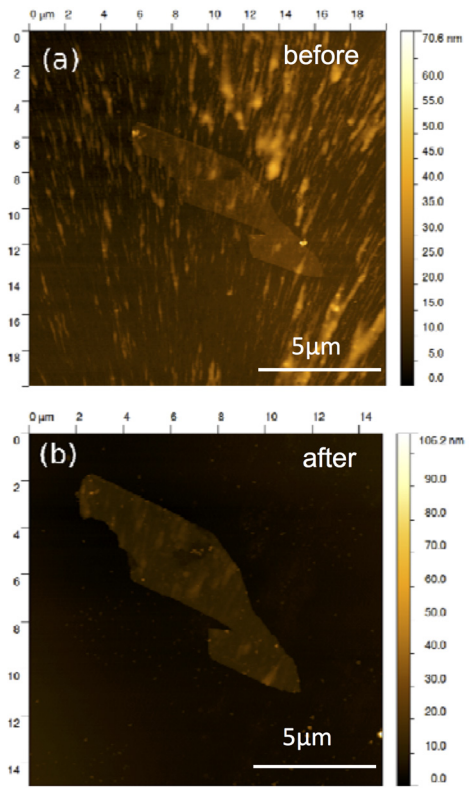

FIG. 2. AFM images of a typical MoS_2 flake (a) before and (b) after exposure to remotely generated oxygen plasma.

Also evident from the *I*–*V* characteristics of Figure 1(c), is the reduction of the sub-threshold gate-voltage swing (S) after treatment with oxygen plasma. The sub-threshold swing is defined as the change in gate voltage required to reduce the current by one decade, i.e., $S = \log(10) \cdot \frac{dV_G}{d(\log(I_D))}$, where the derivative $dV_G/d(\log(I_D))$ is taken at the onset of current. In conventional FETs, sub-threshold transport is dominated by carrier diffusion, and the sub-threshold swing is largely determined by the MOS capacitance, given by the expression $S = \log(10) \cdot \frac{dV_G}{d(\log(I_D))} \approx \frac{kT}{q}\log(10)\left(1 + \frac{C+C_D+C_{it}}{C}\right)$. Here, C is the oxide (back-gate) capacitance,[21] C_D is the depletion layer capacitance, and C_{it} is the capacitance associated with the interface trap charges. From the data in Figure 1, we obtain values of 5.26 V/dec and 3.05 V/dec for the sub-threshold swing before and after oxygen plasma treatment, respectively. This reduction in sub-threshold swing too may be understood as a consequence of the reduction in interfacial charge density, arising primarily due to Sulfur vacancies. The two-fold improvement in sub-threshold voltage swing is important for efficient device operation, as it enables efficient switching the FET state (on/off) at low voltages, and hence minimizes power dissipation.

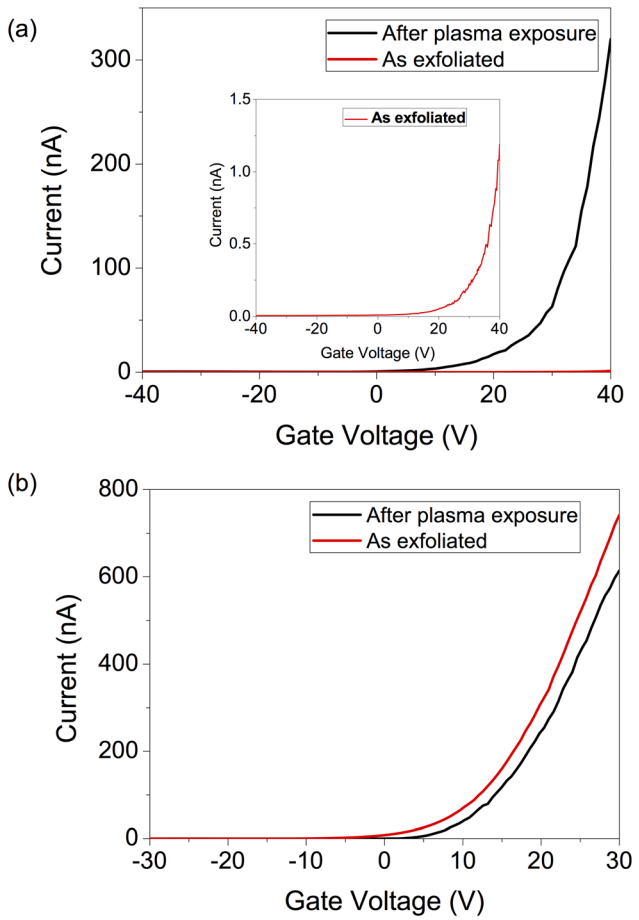

FIG. 3. (a) Current–gate voltage characteristics of a device showing a significant (200X) increase in the field effect carrier mobility after a 3 min exposure to O_2 plasma. The inset shows the *I*–*V* curve before plasma exposure. Figure S4 shows the same data on a log scale. (b) *I*–*V* curve of another device showing a 15% drop in carrier mobility after a 3 min exposure to O_2 plasma.

The field effect mobility of our devices is obtained from the transconductance data shown in Figure 3 using the expression $\mu = \left[\frac{dI_D}{dV_G}\right] \cdot \frac{L}{WCV_{DS}}$, where W and L are the channel width and length, respectively, C is the back gate capacitance, V_G is the gate voltage, V_{DS} is the bias (source-drain) voltage, and I_D is the current flowing through the channel. Here, the derivative dI_D/dV_G is taken at the steepest point on the I–V curve from Figure 3. Although this observed device mobility can depend on various factors, such as contact resistance, and surface interactions, looking at Table I, we observe two distinct trends in the change in mobility due to plasma treatment. For devices in Table I, showing moderate carrier mobilities ($\sim$10 to 100 cm^2/V s), the mobility is typically slightly reduced (by approximately a factor of 2) due to the plasma treatment, indicating that exposure to oxygen plasma does introduce some disorder in the MoS_2 lattice. However, devices with relatively poor carrier mobilities ($\sim$0.001 cm^2/V s) in Table II show significantly enhanced carrier mobilities after plasma treatment. These devices also happened to be fabricated using thinner flakes of MoS_2, where surface scattering is expected to play a more significant role. The low motilities in these devices also indicate they suffer from strong extrinsic scattering effects, such as the presence of tape residue on the MoS_2 surface, rendering them useless. On average, we observe a 75-fold improvement in device mobility for such "damaged" devices, as summarized in Table II. We attribute this dichotomy in trends to the competing effects of oxygen plasma exposure on the MoS_2 surface. While removal of surface impurities from the surface of "damaged" flakes reduces impurity scattering and improves mobility, the direct bombardment of the MoS_2 flake by plasma creates disorder, and degrades the carrier mobility in thicker flakes where surface effects are not the dominant scattering mechanism. Further, the increase in the "off-state" current, as seen in Figure 1(c), is also likely a consequence of an increased density of electronic states within the MoS_2 band gap. Here, the use of a remotely generated plasma minimizes the latter effect, allowing the removal of impurities, without significantly increasing the defect density. However, the use of longer etching times (over 4 min), or larger RF powers, typically does damage the MoS_2 flake itself, with thinner flakes being more susceptible to degradation.

While the same processing steps were used to fabricate all of the devices in this study, we found that the lowest mobility transistors ($\mu < 0.1$ cm^2/V s) show signs of organic residue on the surface, as shown in the AFM image in Figure 2. This indicates that the mobility in these cases is not limited by intrinsic processes (such as defect or phonon scattering in the MoS_2), but rather scattering from the extrinsic contaminant species. Thus, these devices show enhanced carrier mobilities due to the removal of surface residue through plasma treatment. It is known that MoS_2 transistors are also afflicted by surface contaminants and charged impurities, which dope the material n-type[19] and move the turn-on voltage away from zero applied gate voltage. The oxygen plasma consists of negatively charged ions of oxygen and nitrogen, as well as charge neutral free radicals. We believe that these ions and radicals from the plasma bind preferentially to the S-vacancy sites in MoS_2, mitigating the doping effects associated with the vacancy. This reduces the net charge on the defect sites, thereby reducing their effect on the turn-on voltage. The optimal etch time of 2–3 min corresponds to the amount of time needed to "saturate" all the charged impurity sites. Any further increase in exposure time does not lower the turn-on voltage.

For the particular device shown in Figure 3(a), which was seemingly damaged upon fabrication, $W = L = 4$ μm and $C = 11.5$ nF/cm^2 (for a 300 nm SiO_2 back gate). The estimated mobility of the as-fabricated FET device is 0.017 cm^2/V s, which is considerably lower than the typically reported values in literature. However, after treatment with the remote oxygen plasma, the carrier mobility is found to increase to 3.21 cm^2/V s, which is comparable to typical values reported in literature.[4] While most reports in the literature focus on clean FET devices showing higher mobility, our work demonstrates a method to improve even the very worst fabricated devices. In contrast, Figure 3(b) shows the I–V_G characteristics of another MoS_2 device not limited by extrinsic scattering mechanisms. Here, the carrier mobility drops by 16% from 19.8 cm^2/V s to 16.6 cm^2/V s after the 3 min oxygen plasma exposure.

Interestingly, we observe that exposure to remote oxygen plasma is also accompanied by an increase in the hysteresis of the I–V_G characteristics, as shown in Figure S3 of the supplementary material. Previous studies on organic transistors,[22] inorganic semiconductors,[23] as well as carbon nanotubes[24] have shown that hysteresis is a consequence of a dynamic gating of the channel due to mobile surface charges, which may move upon the application of an external field, thereby changing the charge neutrality point. The increased hysteresis is similarly attributed to the dynamic gating caused by adsorption of oxygen plasma species onto the MoS_2 surface. As reported in our previous work, this oxygen plasma treatment improved the luminescence efficiency of few-layer MoS_2 by up to 20-fold due to an indirect-to-direct bandgap transition.[17,25,26] In addition, the photoluminescence linewidth becomes substantially narrower after plasma treatment, as shown in Figure 4. The photoluminescence spectra allow one to determine the relative lifetime of the excitons, whereas transport measurements give a relative measure of the free carrier lifetimes. In transition metal dichalcogenides, there is a dramatic change in the band structure of the materials, as layer thickness is increased above one monolayer. While the most pronounced aspect of this change is the transition to an indirect gap semiconductor in multilayer TMDCs, this change also has a bearing on the selection rules for allowed intervalley scattering processes in monolayer MoS_2. Hence, the PL spectral linewidth is found to be narrower in monolayer MoS_2 than in multilayer MoS_2. Since the exposure to oxygen plasma is also shown to decouple the individual layers, leading to a monolayer-like bandstructure, a similar effect is seen in our spectra. This direct gap transition is highly desirable for applications in optoelectronic devices and, coupled with the improved FET device performance, could pave the way for next generation TMDC based devices. It should be noted that the chemical reaction

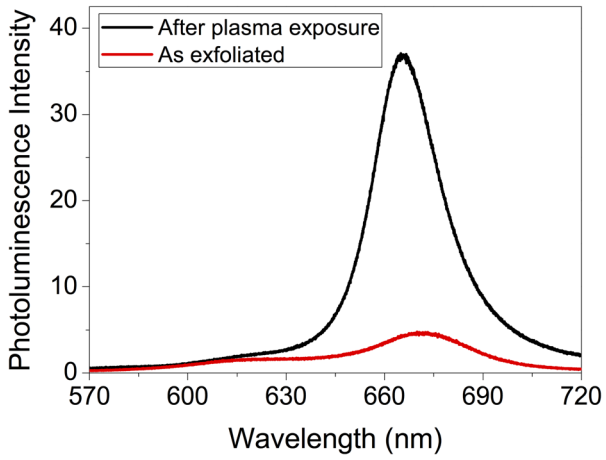

FIG. 4. Enhanced photoluminescence emission from a four layer thick MoS_2 after exposure to remotely generated oxygen plasma.

induced by the O-plasma treatment is permanent and stable, and these devices do not revert to their original *I–V* characteristics over time. The plasma treatment, however, does result in an interlayer decoupling, and some delamination of the MoS_2 is observed when stored under ambient conditions over the span of a few weeks. Therefore, some strategy for hermetic sealing will have to be implemented in order to overcome this instability in practical device applications.

CONCLUSIONS

In summary, we demonstrate a reliable and scalable method using an oxygen plasma treatment to dramatically reduce the turn-on voltage required for switching operation in MoS_2 transistors and simultaneously improve the subthreshold swing of these devices; both are key parameters for enabling low-power electronic devices and sensing applications. The key novelty in this work lies in bringing MoS_2 FETs close to charge neutrality, presumably through the passivation of charged Sulfur vacancies, which typically *n*-dope exfoliated MoS_2.

Estimating the relative importance of various scattering mechanisms (e.g., surface impurities, defects, and phonons) requires a more detailed temperature dependent study of the transport characteristics. However, in our work we observe the following trends:

1. Thin MoS_2 flakes (1–2 layers) are more easily damaged by the oxygen plasma treatment. It is possible to still achieve improved FET performance with the oxygen plasma treatment, but the exposure time and pressure need to be controlled more carefully.
2. Devices with thicker flakes (3–5 layers) are more robust to oxygen plasma exposure, and yet are significantly impacted by the presence of surface impurities. These are the devices that yield both turn-on gate voltages closer to 0 V, as well as increase in carrier mobility, especially in cases where the device performance is limited by extrinsic scattering mechanisms.
3. Thick MoS_2 flakes (>5 layers) also exhibit turn-on gate voltages far from 0 V. However, their device mobilities are less prone to scattering from surface impurities. Hence, after exposure to the remote oxygen plasma, we see a shift of the charge neutrality point toward zero applied gate voltage, but moderate reduction of carrier mobility is also observed.

Lithographically fabricated FETs also suffer from non-uniformities and huge variability in device-to-device performance, which is greatly reduced upon exposure to the remote oxygen plasma. Our results also shed light on the role of defect and impurity scattering mechanisms limiting device mobilities in MoS_2 transistors. While this result is not meant to compete with other methodologies used to make high mobility FET devices, such as using suspended MoS_2 or MoS_2 sandwiched between two flakes of boron nitride, it provides a scalable route for creating moderate-mobility MoS_2 FETs with lower subthreshold swing and turn-on voltages, while significantly reducing the device-to-device variability.

SUPPLEMENTARY MATERIAL

See supplementary material for additional data regarding the influence of the metal-semiconductor contact, as well for as a comparison with results from existing literature.

ACKNOWLEDGMENTS

This research was supported by the Department of Energy (DOE) Award No. DE-FG02–07ER46376 (Z. L.) and NSF Award No. 1402906 (R.D.).

[1]K. F. Mak, C. Lee, J. Hone, J. Shan, and T. F. Heinz, Phys. Rev. Lett. **105**, 136805 (2010).
[2]K. F. Mak, K. L. He, J. Shan, and T. F. Heinz, Nat. Nanotechnol. **7**, 494 (2012).
[3]H. L. Zeng, J. F. Dai, W. Yao, D. Xiao, and X. D. Cui, Nat. Nanotechnol. **7**, 490 (2012).
[4]B. Radisavljevic, A. Radenovic, J. Brivio, V. Giacometti, and A. Kis, Nat. Nanotechnol. **6**, 147 (2011).
[5]A. Splendiani, L. Sun, Y. Zhang, T. Li, J. Kim, C.-Y. Chim, G. Galli, and F. Wang, Nano Lett. **10**, 1271 (2010).
[6]K. S. Novoselov, A. K. Geim, S. V. Morozov, D. Jiang, M. I. Katsnelson, I. V. Grigorieva, S. V. Dubonos, and A. A. Firsov, Nature **438**, 197 (2005).
[7]Q. H. Wang, K. Kalantar-Zadeh, A. Kis, J. N. Coleman, and M. S. Strano, Nat. Nanotechnol. **7**, 699 (2012).
[8]S. Kim *et al.*, Nat. Commun. **3**, 1011 (2012).
[9]Y. J. Zhang, T. Oka, R. Suzuki, J. T. Ye, and Y. Iwasa, Science **344**, 725 (2014).
[10]R. Cheng *et al.*, Nano Lett. **14**, 5590 (2014).
[11]Y. Yoon, K. Ganapathi, and S. Salahuddin, Nano Lett. **11**, 3768 (2011).
[12]Y. Liu *et al.*, Nano Lett. **15**(5), 3030–3034 (2015).
[13]X. Cui *et al.*, Nat. Nanotechnol. **10**, 534–540 (2015).
[14]M. S. Choi, G. H. Lee, Y. J. Yu, D. Y. Lee, S. H. Lee, P. Kim, J. Hone, and W. J. Yoo, Nat. Commun. **4**, 1624 (2013).
[15]G. H. Lee *et al.*, ACS Nano **7**, 7931 (2013).
[16]J. S. Ross *et al.*, Nat. Nanotechnol. **9**(4), 268–272 (2014).
[17]R. Dhall, M. R. Neupane, D. Wickramaratne, M. Mecklenburg, Z. Li, C. Moore, R. K. Lake, and S. Cronin, Adv. Mater. **27**, 1573 (2015).
[18]M. Amani *et al.*, Science **350**, 1065 (2015).
[19]C.-P. Lu, G. Li, J. Mao, L.-M. Wang, and E. Y. Andrei, Nano Lett. **14**, 4628 (2014).

[20]M. R. Islam, N. Kang, U. Bhanu, H. P. Paudel, M. Erementchouk, L. Tetard, M. N. Leuenberger, and S. I. Khondaker, Nanoscale **6**, 10033 (2014).
[21]S. M. Sze and K. K. Ng, *Physics of Semiconductor Devices* (John Wiley & Sons, 2006).
[22]G. Gu and M. G. Kane, Appl. Phys. Lett. **92**, 053305 (2008).
[23]J. Goldberger, D. J. Sirbuly, M. Law, and P. Yang, J. Phys. Chem. B **109**, 9 (2005).
[24]W. Kim, A. Javey, O. Vermesh, Q. Wang, Y. Li, and H. Dai, Nano Lett. **3**, 193 (2003).
[25]Z. Li, S. Yang, R. Dhall, E. Kosmowska, H. Shi, I. Chatzakis, and S. B. Cronin, ACS Nano **10**(7), 6836–6842 (2016).
[26]R. Dhall, K. Seyler, Z. Li, D. Wickramaratne, M. R. Neupane, I. Chatzakis, E. Kosmowska, R. K. Lake, X. Xu, and S. B. Cronin, ACS Photonics **3**(3), 310–314 (2016).